

PAPER • OPEN ACCESS

Vibration-based system identification of a large steel box girder bridge

To cite this article: R Schneider *et al* 2024 *J. Phys.: Conf. Ser.* **2647** 182039

View the [article online](#) for updates and enhancements.

You may also like

- [Discussion on manufacturing technology of steel box girder of cross-line bridge engineering in Xiamen Hele road](#)
Zhengwei Feng and Longbin Lin
- [Analysis on ductility and energy dissipation performance of steel box column-beam irregular joint](#)
Zongbo Hu
- [Walking-Type Bidirectional Incremental Launching and Mid-Span Closure Technology for Steel Box Girders with Long Cantilevers](#)
Kai Wang, Wei Lu and Zhongbiao Zhang

PRIME
PACIFIC RIM MEETING
ON ELECTROCHEMICAL
AND SOLID STATE SCIENCE

HONOLULU, HI
October 6-11, 2024

Joint International Meeting of
The Electrochemical Society of Japan (ECSJ)
The Korean Electrochemical Society (KECS)
The Electrochemical Society (ECS)

Early Registration Deadline:
September 3, 2024

MAKE YOUR PLANS NOW!

Vibration-based system identification of a large steel box girder bridge

R Schneider*, P Simon, F Hille, R Herrmann and M Baeßler

Bundesanstalt für Materialforschung und -prüfung (BAM), Unter den Eichen 87,
12205 Berlin, Germany

* Corresponding author: ronald.schneider@bam.de

Abstract. The Bundesanstalt für Materialforschung und -prüfung (BAM) collaborates with TNO to develop a software framework for automated calibration of structural models based on monitoring data. The ultimate goal is to include such models in the asset management process of engineering structures. As a basis for developing the framework, a multi-span road bridge consisting of ten simply supported steel box girders was selected as a test case. Our group measured output-only vibration data from one box girder under ambient conditions. From the data, we determined eigenfrequencies and mode shapes. In parallel, we developed a preliminary structural model of the box girder for the purpose of predicting its modal properties. In this contribution, we provide an overview of the measurement campaign, the operational modal analysis, the structural modeling and qualitatively compare the identified with the predicted modes. As an outlook, we discuss the further steps in the calibration process and future applications of the calibrated model.

1. Introduction

Structural health monitoring (SHM) systems provide information on the demands structures are subject to, their condition and their performance. This information can be used to reduce uncertainties in engineering models, improve predictions of the condition and performance and optimize the structural integrity management. A consistent framework for calibrating engineering models with data and observations is Bayesian updating [e.g., 1, 2]. However, this approach will only enhance the structural integrity management in practice if efficient and robust software is developed that can be used by engineers who are not experts in the field. For this reason, researchers at BAM and TNO are collaborating to develop a software tool for automated calibration of structural models using Bayesian methods.

A multi-span road bridge shown in Figure 1 (top) was selected as a real-world application to test the software tool. As part of the project, a multi-setup operational modal analysis of one of the bridge spans was performed to determine its dynamic properties in terms of natural frequencies and mode shapes. This information will be used as a basis for calibrating a structural model of the bridge span. In this contribution, we summarize the measurements and operational modal analysis (OMA). In addition, we briefly describe the development of an initial structural model and compare the “measured” with the model predicted dynamic properties. We conclude the paper with a discussion on the subsequent steps in the calibration process and provide an outlook on the possible applications of the calibrated model.



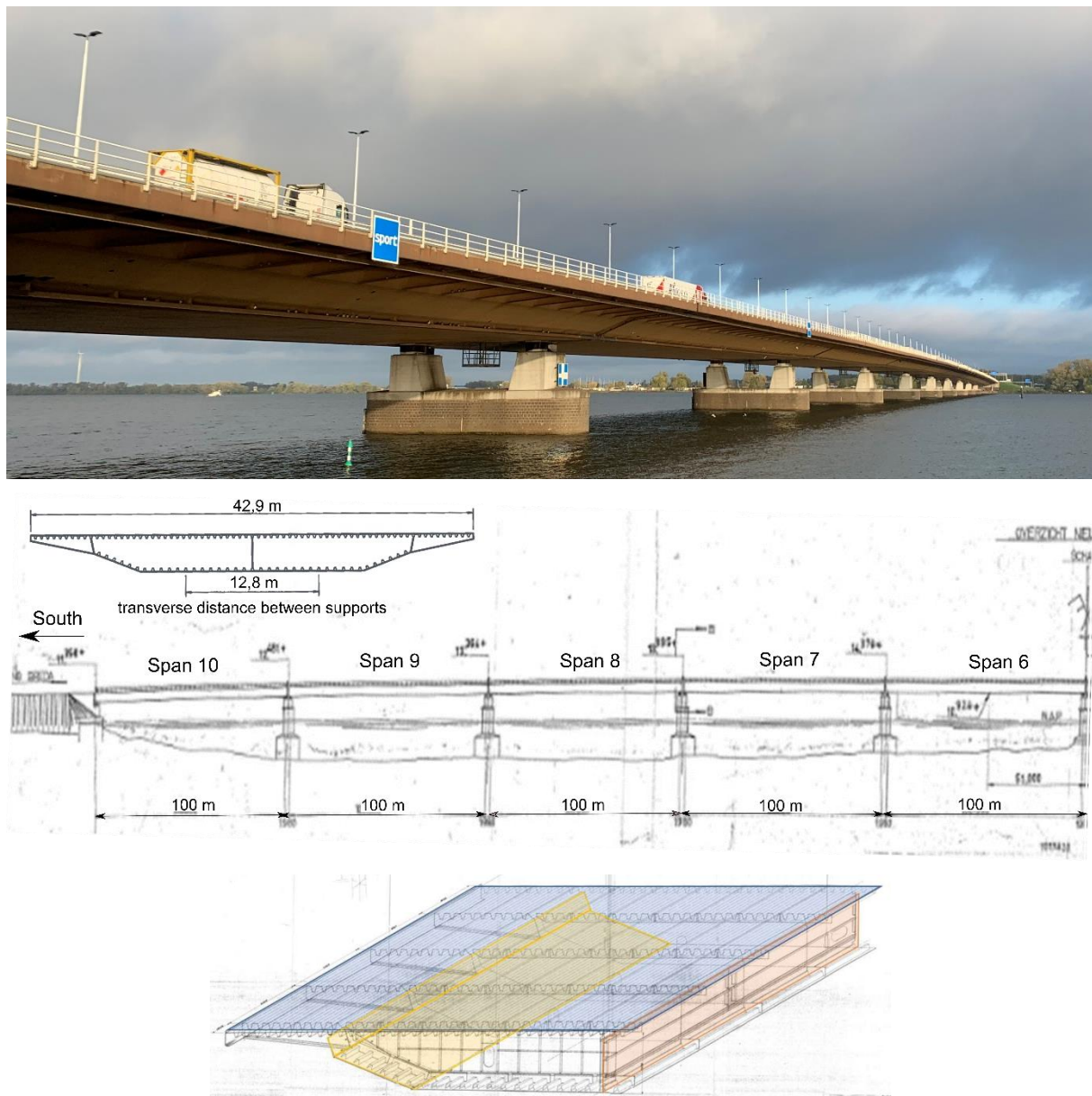


Figure 1. Top: Road bridge consisting of ten simply supported steel box girders. Center: Elevation of the southern half of the bridge together with an illustration of the cross section of the box girder. Bottom: Half of a regular segment of the box girder. Transverse bulkheads are spaced at 4.17 m intervals and a longitudinal bulkhead is located at the centerline of the box girder.

2. Description of the bridge

The road bridge is approximately 1 km long and comprises ten spans of approximately 100 m (see Figure 1, center). In each direction, the bridge consists of five lanes including an emergency and a cycling lane. The primary structure of each span is a simply supported steel box girder with a symmetrical cross section (see Figure 1, center). The maximum depth of the girder is 3.5 m and its deck plate is 42.9 m wide. Along the longitudinal axis, each girder is composed of five regular segments of 16.67 m and two end segments of 7.29 m and 9.38 m. The deck plate, webs and bottom plate of the box girder are orthotropic steel plates with trapezoidal stiffeners (see Figure 1, center). Along the box girder, transverse bulkheads are typically spaced at 4.17 m intervals and a longitudinal bulkhead is located at its centerline (see Figure 1, bottom). In longitudinal direction, the distance between the supports is 100 m

and in transverse direction 12.8 m (see Figure 1, center). In 2005, a high strength concrete overlay of approximately 7 cm was applied to the orthotropic deck plate to mitigate fatigue damage due to the increased traffic load.

3. Ambient vibration measurements

In October 2022, we performed output-only vibration measurements under ambient conditions as a basis of an OMA of the southernmost box girder (span 10, see Figure 1, center). The measurements were conducted in three stages using a 30-channel system with 25 vertical geophones (vibration velocity sensors), four horizontal geophones and one vertical force balance accelerometer. In each stage, a different sensor setup was applied as illustrated in Figure 2. All setups had some reference sensors with fixed positions in common while the position of 18 vertical geophones was changed from setup to setup (see Figure 2, top). Two reference sensors were placed at the southern supports of the box girder. The remaining reference sensors were placed on the bottom plate of the box girder at the positions indicated in Figure 2 (top). In setup 1 and 3 (western and eastern side of the box girder), the 18 vertical geophones with changing positions were placed on the top horizontal stiffener of the corresponding transverse bulkheads (see Figure 2, bottom left). In setup 2 (centerline of the box girder), these sensors were positioned on the bottom plate as shown in Figure 2 (bottom left). All sensors were mounted on base plates with three conical pins (see Figure 2, bottom right). For each sensor setup, a 60-minute record of geophone data and accelerations was measured at a sampling rate of 1000 Hz.

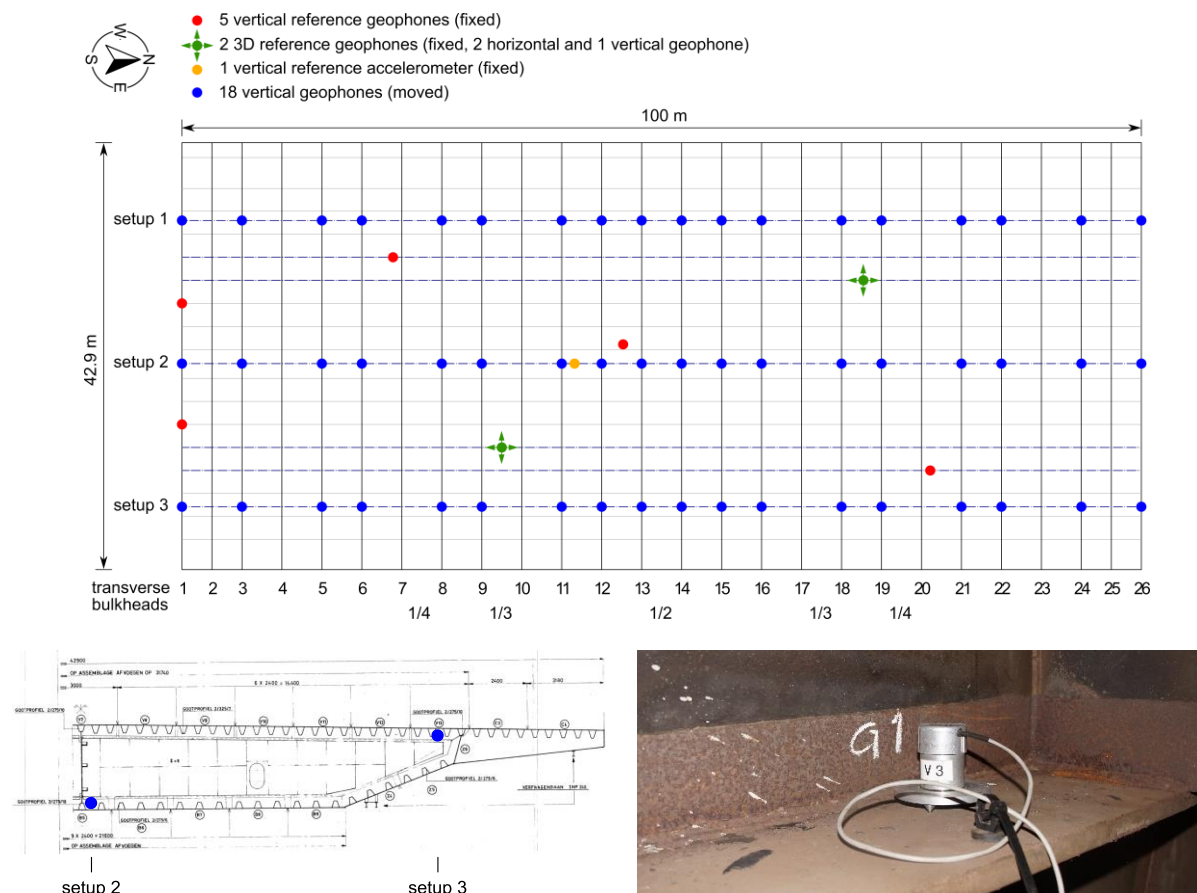


Figure 2. Top: Plan view of the deck plate of the box girder indicating the positions of the reference sensors and the geophones, whose position was changed from setup to setup. Bottom left: Vertical position of the non-fixed geophones in setup 2 and 3. Bottom right: Vertical geophone mounted on a base plate with three conical pins.

4. Operational modal analysis

In the current contribution, natural frequencies and mode shapes of the southernmost box girder (span 10) were determined based on the measured geophone signals. As a first step, each individual geophone signal was filtered using a bandpass Butterworth filter of order 8 with cutoff frequencies of 0.75 Hz and 300 Hz, where the upper cutoff frequency was chosen to prevent aliasing. In the second step, the individual geophone signals were transformed to the frequency domain and calibrated as follows:

$$S'[f] = \frac{S[f]}{T[f]} \quad (1)$$

where $S[f]$ is the Fourier-transform of the raw signal in [V], $T[f]$ is the complex-valued transfer function for each frequency f and $S'[f]$ is the Fourier-transform of the calibrated signal in [m/s]. Subsequently, the calibrated signals were transformed back into the time domain. The transfer function for each geophone were measured at 24 different frequencies using a shaker and laser vibrometer. An example of such a measured transfer function is shown in Figure 3. Based on the measured transfer functions, $T[f] = \text{sensitivity}[f] \cdot \exp(i \cdot \text{phase}[f])$ was constructed by interpolation. Note that the lowest frequency considered in the measurement of the transfer function was 0.75 Hz. This value was also chosen as the lower cutoff frequency of the applied bandpass filter (see above).

In the third step, the calibrated geophone signals from the different measurement setups were merged and normalized. Finally, the natural frequencies and mode shapes were determined by applying the frequency domain decomposition (FDD) technique [3] in conjunction with peak picking. The third and fourth step were performed using ARTeMIS Modal [4].

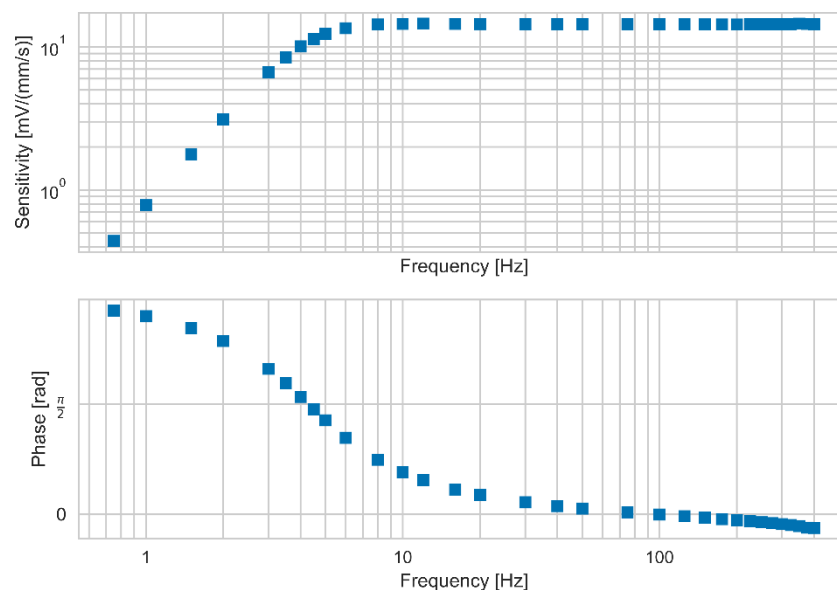


Figure 3. Example of a measured transfer function of a geophone.

5. Structural modeling

A linear-elastic finite element (FE) model of the box girder was developed by BAM in ANSYS Mechanical APDL [5] for the purpose of predicting eigenfrequencies and mode shapes (see Figure 4). The deck plate, webs, bottom plate and bulkheads were modeled with shell elements. The trapezoidal stiffeners of all orthotropic plates were modeled as eccentric beam elements. Stiffeners of and openings in the bulkheads were not included in the model. The concrete overlay was captured in the model by describing the deck plate with composite shell elements. This modeling approach assumes perfect bonding between the steel deck and the concrete overlay. The properties of the ANSYS model were

defined based on information collected during the measurement campaign, design drawings, assessment reports and a highly detailed DIANA [6] model provided by TNO. The DIANA model was developed to compare predicted strains with strains measured during load tests. The additional ANSYS model was developed by BAM because the high level of detail provided by the DIANA model is not required in the prediction of the modal properties.

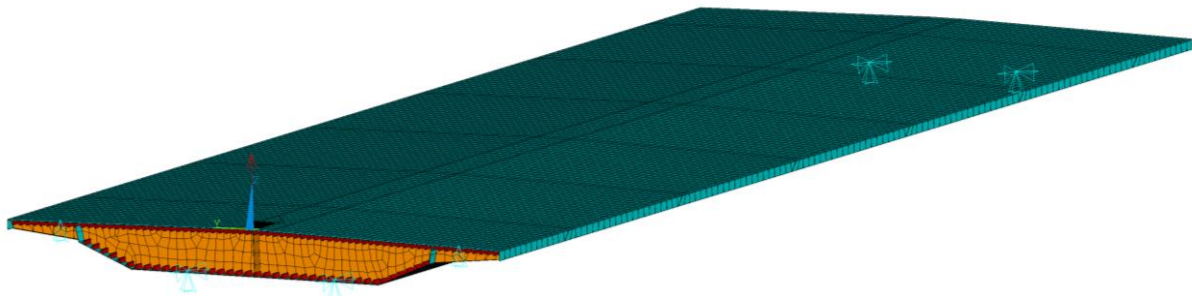


Figure 4. Illustration of the ANSYS model of the steel box girder.

6. Results

Figure 5 shows the FDD singular value decomposition (SVD) plot for the frequency range 0.75 Hz to 10.5 Hz. From this plot, nine modes were identified using peak picking.

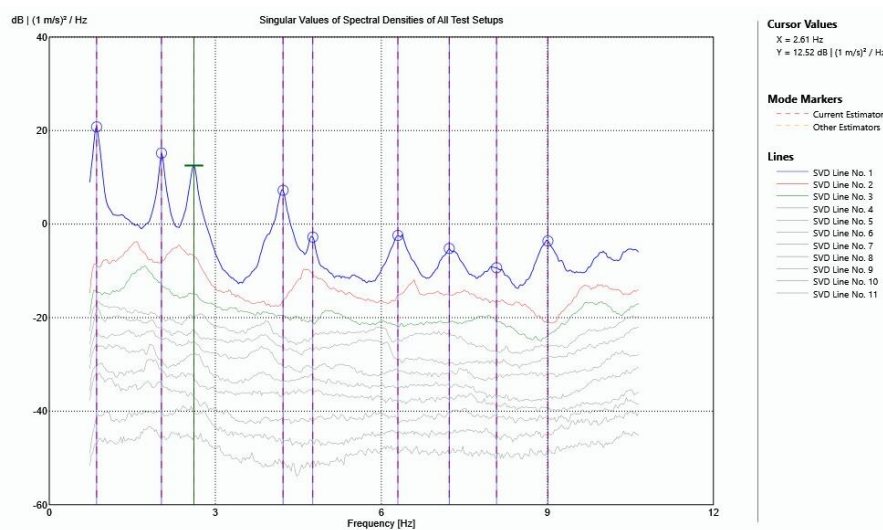


Figure 5. FDD singular value decomposition (SVD) plot together with picked peaks.

The identified modes in terms of natural frequencies and mode shapes are summarized in Table 1. At the current stage, these modes were qualitatively matched with modes obtained from the modal analysis of the ANSYS model. The matched numerical modes are also provided in Table 1. The identified and matched numerical mode shapes appear to correspond well. At this point, this is a purely qualitative assessment and in the future the consistency between the identified and predicted mode shapes will be quantitatively assessed, for example, based on the modal assurance criterion [7].

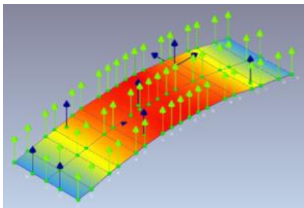
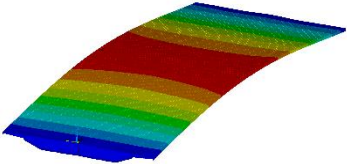
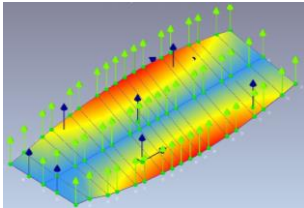
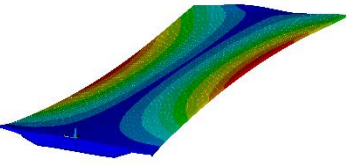
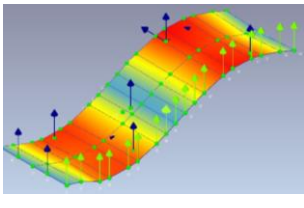
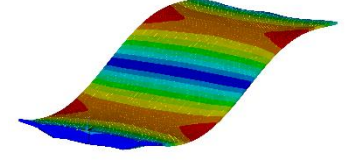
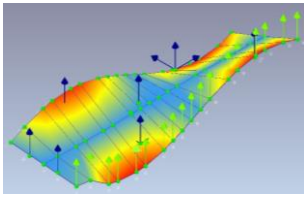
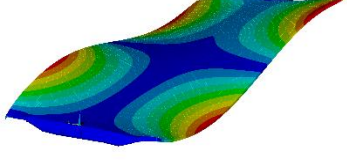
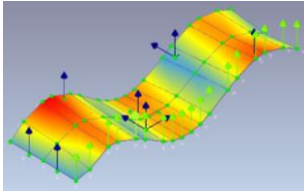
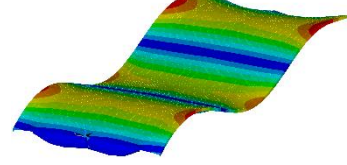
The discrepancies between the frequencies of the identified and numerical modes indicate that the ANSYS model may have to be enhanced to include, for example,

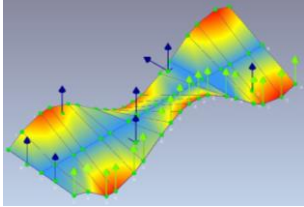
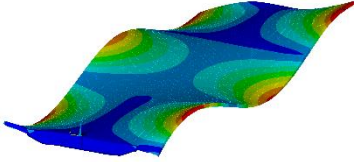
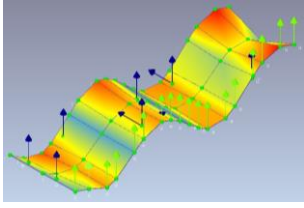
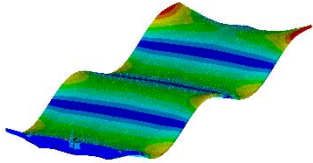
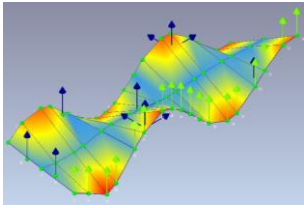
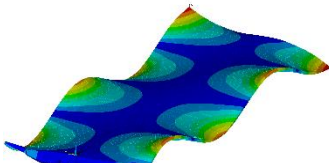
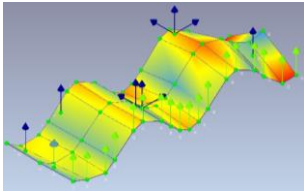
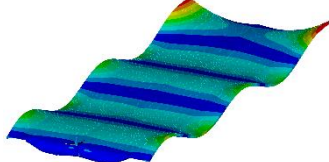
- an improved model of the spatially varying concrete overlay,
- improved models of the support conditions,
- attachments such as parapets and crash barriers, and

- the asphalt layer on both cycling lanes and the center strip of the bridge.

In addition, the parameters of the ANSYS model will have to be calibrated based on the identified modal properties using probabilistic (and deterministic) model updating techniques [e.g., 8].

Table 1. Comparison of the identified modes with the (qualitatively) matched numerical modes.

	Identified modes	Matched numerical modes
1	0.85 Hz 	0.99 Hz 
2	2.03 Hz 	1.80 Hz 
3	2.61 Hz 	2.60 Hz 
4	4.22 Hz 	3.78 Hz 
5	4.76 Hz 	4.70 Hz 

	Identified modes	Matched numerical modes
6	6.30 Hz 	5.82 Hz 
7	7.23 Hz 	6.67 Hz 
8	8.08 Hz 	7.58 Hz 
9	9.00 Hz 	8.54 Hz 

7. Concluding remarks

To obtain data from a real bridge structure, the vibration response of one of the simply supported spans of a road bridge was measured under ambient conditions. The recorded data were analyzed using operational modal analysis techniques to identify its modal properties. This information will be applied to test a software tool that enables the calibration of structural models using Bayesian methods. To this end, an initial structural model of the bridge span was developed. A qualitative comparison of the identified modal properties with the model predicted properties highlights that the model has to be enhanced and calibrated to minimize the difference between the identified and predicted modal properties.

As a next step, the simulation model will be parameterized, and a prior probabilistic model of the model parameters will be proposed. The set of parameters will be defined such that model uncertainties and the uncertainties in the identified modal properties can also be learned during the calibration. Since FE models are generally computationally expensive, it may be necessary to develop a surrogate model based on the probabilistic FE model to enable efficient Bayesian updating of the probabilistic model of the model parameters [e.g., 9]. As part of the software test, different Bayesian inference algorithms will be applied, and their performance compared. In addition, deterministic model updating techniques [e.g.,

10] will be utilized to enable a comparative assessment of the performance of deterministic and probabilistic approaches.

The model parameters, which are calibrated based on the identified modal properties, can potentially be used as a basis for predicting the fatigue life of the box girder. To this end, the updated probabilistic model of the model parameters can be applied as input to a structural model specifically developed for the purpose of predicting stresses at the critical fatigue hotspots in conjunction with a site-specific traffic load model [11]. Based on the simulated hotspot stress histories and available inspection results, hotspot fatigue models and predictions of the fatigue life can be updated [e.g., 12]. This information can subsequently be applied to support decisions on future maintenance actions. In addition, the calibrated model can be utilized to (a) evaluate the performance of damage detection methods [e.g., 13] based on simulated damage processes and monitoring outcomes and (b) optimize SHM systems using value of information analysis [14, 15].

Acknowledgements

We gratefully acknowledge Rijkswaterstaat for the opportunity to use the bridge as a test case and TNO's support in preparing and conducting the vibration measurements and building the ANSYS model.

References

- [1] P. Simon, R. Schneider, E. Viefhues, S. Said, R. Herrmann, and M. Baeßler, "Vibration-based structural health monitoring of a reinforced concrete beam subject to varying ambient temperatures using Bayesian methods," presented at the XI International Conference on Structural Dynamics (EURODYN 2020), Athens, Greece, 23-25 November, 2020.
- [2] P. Simon, R. Schneider, and M. Baeßler, "Bayesian system identification of a reinforced concrete beam subject to temperature variations based on static response data," presented at the 10th International Conference on Bridge Maintenance, Safety and Management (IABMAS 2020), Sapporo, Japan, 11-15 April, 2021. Available: <https://opus4.kobv.de/opus4-bam/frontdoor/index/index/docId/52809>.
- [3] B. Rune, Z. Lingmi, and A. Palle, "Modal identification of output-only systems using frequency domain decomposition," *Smart Materials and Structures*, vol. 10, no. 3, p. 441, 2001, doi: <https://dx.doi.org/10.1088/0964-1726/10/3/303>.
- [4] Structural Vibration Solutions A/S. "ARTEMIS Modal." <https://svibs.com/artemis-modal/> (accessed 2023).
- [5] Ansys Inc. "Ansys 2021 R2: What's New with Ansys Mechanical." <https://www.ansys.com/de-de/resource-center/webinar/ansys-2021-r2-whats-new-with-ansys-mechanical> (accessed 2023).
- [6] DIANA FEA BV. "DIANA FEA." <https://dianafea.com/index.php/> (accessed 2023).
- [7] M. Brehm, V. Zabel, and C. Bucher, "An automatic mode pairing strategy using an enhanced modal assurance criterion based on modal strain energies," *Journal of Sound and Vibration*, vol. 329, no. 25, pp. 5375-5392, 2010, doi: <https://doi.org/10.1016/j.jsv.2010.07.006>.
- [8] E. Simoen, G. De Roeck, and G. Lombaert, "Dealing with uncertainty in model updating for damage assessment: A review," *Mechanical Systems and Signal Processing*, vol. 56-57, pp. 123-149, 2015, doi: <https://doi.org/10.1016/j.ymsp.2014.11.001>.
- [9] B. Sudret, S. Marelli, and J. Wiart, "Surrogate models for uncertainty quantification: An overview," presented at the 11th European Conference on Antennas and Propagation (EUCAP), 2017.
- [10] H. T. M. Luong, V. Zabel, W. Lorenz, and R. G. Rohrmann, "Vibration-based Model Updating and Identification of Multiple Axial Forces in Truss Structures," *Procedia Engineering*, vol. 188, pp. 385-392, 2017, doi: <https://doi.org/10.1016/j.proeng.2017.04.499>.
- [11] J. Maljaars, "Evaluation of traffic load models for fatigue verification of European road bridges," *Engineering Structures*, vol. 225, p. 111326, 2020, doi: <https://doi.org/10.1016/j.engstruct.2020.111326>.

- [12] J. Maljaars and A. C. W. M. Vrouwenvelder, "Probabilistic fatigue life updating accounting for inspections of multiple critical locations," *International Journal of Fatigue*, vol. 68, pp. 24-37, 2014.
- [13] E. Viefhues, M. Döhler, F. Hille, and L. Mevel, "Statistical subspace-based damage detection with estimated reference," *Mechanical Systems and Signal Processing*, vol. 164, p. 108241, 2022, doi: <https://doi.org/10.1016/j.ymssp.2021.108241>.
- [14] A. Kamariotis, E. Chatzi, and D. Straub, "A framework for quantifying the value of vibration-based structural health monitoring," *Mechanical Systems and Signal Processing*, vol. 184, p. 109708, 2023, doi: <https://doi.org/10.1016/j.ymssp.2022.109708>.
- [15] L. Eichner, R. Schneider, P. Simon, and M. Baeßler, "Optimal sensor placement for vibration-based structural health monitoring obtained via value of information analysis as part of a digital structural integrity management of offshore structures," presented at the 3rd International Conference on Health Monitoring of Civil & Maritime Structures (HeaMES 2022), Online, 08.06.2022, 2022.